Annual Review of Analytical Chemistry

SERS Sensors: Recent Developments and a Generalized Classification Scheme Based on the Signal Origin

Xin Gu, Michael J. Trujillo, Jacob E. Olson, and Jon P. Camden

Department of Chemistry and Biochemistry, University of Notre Dame, Notre Dame, Indiana 46556, USA; email: jon.camden@nd.edu

Annu. Rev. Anal. Chem. 2018. 11:13.1–13.23

The *Annual Review of Analytical Chemistry* is online at anchem.annualreviews.org

https://doi.org/10.1146/annurev-anchem-061417-125724

Keywords

surface-enhanced Raman spectroscopy, SERS, surface-affinity strategy, SAS, SERS-tags strategy, STS, probe-mediated strategy, PMS, sensors, nanoparticles

Abstract

Owing to its extreme sensitivity and easy execution, surface-enhanced Raman spectroscopy (SERS) now finds application for a wide variety of problems requiring sensitive and targeted analyte detection. This widespread application has prompted a proliferation of different SERS-based sensors, suggesting the need for a framework to classify existing methods and guide the development of new techniques. After a brief discussion of the general SERS modalities, we classify SERS-based sensors according the origin of the signal. Three major categories emerge from this analysis: surface-affinity strategy, SERS-tag strategy, and probe-mediated strategy. For each case, we describe the mechanism of action, give selected examples, and point out general misconceptions to aid the construction of new devices. We hope this review serves as a useful tutorial guide and helps readers to better classify and design practical and effective SERS-based sensors.

1. INTRODUCTION

The wide-ranging analytical potential of surface-enhanced Raman spectroscopy (SERS) was recognized almost immediately after its discovery in 1977. Fantastic progress toward this potential has been made in the intervening years, and SERS is now applied in diverse fields such as food safety, homeland security, biological sample analysis and imaging, diagnosis, and surface science (1–6). The proliferation of SERS-based sensors in recent years suggests the need for a framework from which to understand the different modalities underlying SERS-based sensors. After beginning with a brief historical perspective and discussion of the key SERS mechanisms, we turn to a detailed categorization of SERS-based sensors. Throughout this review, we endeavor to address common misconceptions and highlight practical considerations for each of the SERS-based schemes discussed.

In 1974, Fleischman et al. (7) observed a large Raman signal from pyridine adsorbed on electrochemically roughened silver surfaces and attributed this enhancement to an increased surface area of the roughened electrodes. In 1977, Albrecht & Creighton (8) and Jeanmaire & Van Duyne (9) independently recognized that the increased signal could not be explained by the surface area alone and therefore proposed the chemical and electromagnetic mechanisms (CM and EM), respectively. These two processes, which are now considered fundamental to the SERS effect, are easily understood using the equation for an induced dipole moment μ:

$$\mu = \alpha E,$$

where α is the polarizability of the molecule, and E is the applied electric field.

The EM applies to both chemisorbed and physisorbed molecules in close proximity (<5 nm) to the metal surface. Moskovits (10, 11) recognized that the large electromagnetic effects arose from excitation of localized surface plasmon resonances (LSPRs), as they provide an amplification of the applied electric field E at the metal surface. SERS-substrates are typically fabricated from the noble metals such as Au and Ag owing to their ability to support visible-wavelength plasmons and their relative inertness (11). This mechanism usually contributes 10^4–10^6 to the enhancement factor (EF) and is the major driver of the SERS effect (12, 13). On the other hand, the CM most commonly arises upon chemisorption of a molecule to the metal surface and the establishment of a charge transfer state between the molecule and metal surface, thereby enhancing the polarizability α of the molecule. However, the EF arising from this phenomenon is usually only one to two orders of magnitude. Interestingly, recent work suggests that two-dimensional materials such as graphene can greatly enhance the Raman signal via the CM (14).

Despite differences in the physics underlying the CM and EM, both have the common critical requirement that the distance between the Raman reporter and the substrate be small, a theme that is highlighted in this review. In the CM case, the Raman reporter should be in direct contact with the substrate. While the distance requirement for the EM is less severe, it still operates most effectively when the Raman reporter is proximal to the SERS substrate (<5 nm). Various experimental approaches have been employed to determine the distance-dependent enhancement, and one commonly used expression for the distance dependent enhancement is given by (15)

$$I_{\mathrm{SERS}} = \left(\frac{a+r}{a}\right)^{-10},$$

where I_{SERS} is the intensity of SERS signal, a is the radius of curvature of the roughness feature on the plasmonic substrate, and r is the distance from the surface. The SERS signal decays exponentially as the molecules move further from the SERS-active surface; therefore, the distance between

the Raman reporter and the substrate is a key factor to consider when constructing SERS-based sensors. Recent work has also highlighted the importance of surface-adsorption equilibria on the overall SERS sensor response (16).

Apart from the proximity effect, many reports indicate that extremely large enhancements can originate from the plasmons formed in the gap region of coupled nanoparticles (NPs) (17). These regions, known as "hotspots," can provide enhancements in excess of 10^9 for molecules located in the NP junction. Taking advantage of the electromagnetic hotspots in aggregated Ag nanoparticles (AgNPs) and resonance Raman scattering, Nie & Emory (18) and Kneipp et al. (19) observed SERS from single rhodamine 6G and crystal violet molecules, respectively, in 1997. The development of SERS-based sensors experienced phenomenal growth (5) after these first reports of single-molecule SERS.

Although SERS-based sensors are relatively new compared to established methods such as fluorescence and electrochemistry, they have gained recognition and popularity among the analytical chemistry community. In addition to its superb sensitivity, SERS also confers other significant advantages: (*a*) SERS is a vibrational spectroscopy; therefore, it provides chemical specificity. (*b*) SERS-based sensors are usually resistant to photobleaching; consequently, they are more suitable for long-term tracking and labeling (20). (*c*) The narrow width (generally 1–2 nm) of a Raman band enables the potential of multiplexing and high-throughput detection (21, 22).

In this review, we organize the large and diverse field of SERS-based sensors according to the origin of the signal generated. In particular, we classify the sensing modalities into three categories (**Figure 1**): (*a*) surface-affinity strategies (SASs), where the signal arises from the analyte; (*b*) SERS-tags strategies (STSs), where the signal arises from the Raman tags; and (*c*) and probe-mediated strategies (PMSs), where the signal arises from a change in the probe upon the interaction with the analyte. In each category, we introduce several subcategories to capture the diversity of current SERS methods. We hope this review provides a framework for discussing the broad field of SERS-based devices and can inspire newcomers to develop SERS-based sensors in a logical, robust, and sensitive manner based on their specific situation.

2. SURFACE-AFFINITY STRATEGIES

We begin with methods that measure Raman scattering arising from the analyte, as they are conceptually the simplest. When employing this approach, the analyte is either directly adsorbed to the SERS-active metal or is captured by a functionalized surface. In either case, the quantification or identification is achieved by measuring the Raman signal from the analyte. When discussing the use of unfunctionalized surfaces, it is important to recognize that NP synthesis methods often yield metal surfaces capped with a charged agent, for example, citrate in the commonly used Lee and Meisel procedure (23). In this section, we consider "synthesized" films and NPs, i.e., without addition or exchange of a ligand, as unfunctionalized. While the preparation of unfunctionalized substrates is facile, their selectivity is severely limited owing to nonspecific binding, and in most cases, a lack of analyte affinity for the metal surface. Nonspecific binding can be addressed by surface functionalization; however, such schemes often suffer from the well-known first-layer effect proposed by Otto and coworkers (24, 25), where the bulk of the scattering signal measured is obtained from the functionalization layer and not the analyte of interest. As the electric field enhancement decays strongly with the distance from the surface, the scattering cross section of the ligand relative to the analyte should be minimized. Despite the challenges, a variety of successful and simple detection schemes based on SAS have been reported.

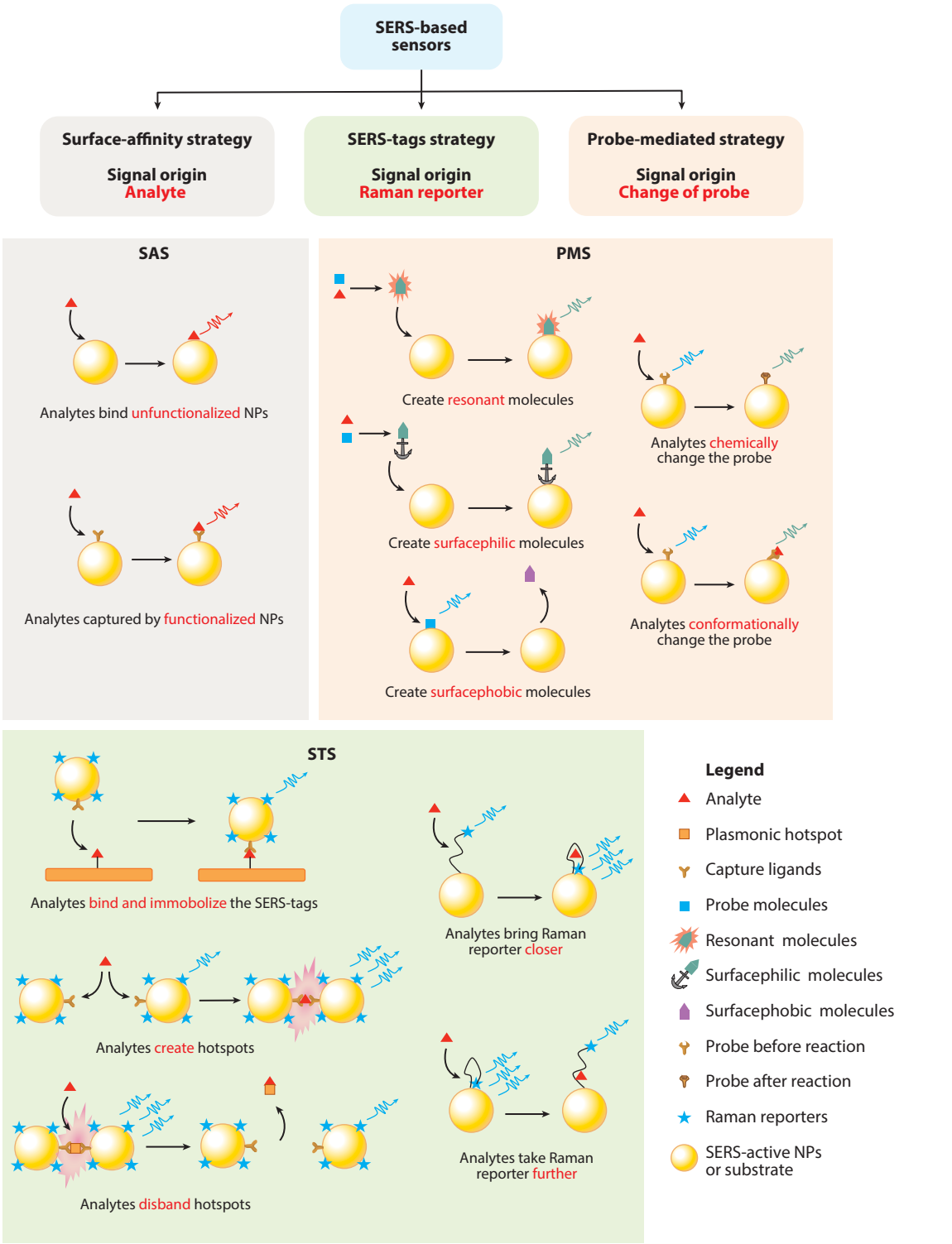

(*Caption appears on following page*)

Figure 1 (*Figure appears on preceding page*)

Schematic figure illustrating the classification scheme of SERS sensors, organized according to the signal origin. The SAS measures the signal directly from the analyte using either unfunctionalized or functionalized substrates. The STS measures the signal from a Raman reporter. The detection is enabled by immobilization of the SERS-tags, modulation of hotspots, or modulation of the distance. The PMS measures the change in the reporter molecules upon the interaction with the analyte. The detection is enabled by the creation of resonance Raman, change in surface affinity, or probe-analyte interaction–induced spectral change. Abbreviations: NP, nanoparticle; PMS, probe-mediated strategy; SAS, surface-affinity strategy; SERS, surface-enhanced Raman spectroscopy; STS, SERS-tag strategy.

2.1. Unfunctionalized Substrates

The simplest detection schemes rely on the native affinity of the analyte for the unmodified SERS substrate. This affinity stems from the fundamental interactions of molecules with surfaces: electrostatic, physisorption (van der Waals), and chemisorption (covalent). Electrostatic interactions enable inorganic ions and charged organic molecules, for example, those containing carboxylates or ammoniums, to adsorb onto metal surfaces. Alternatively, ions such as cyanide (26) and functional groups like thiols (27) can covalently bind to a noble metal surface, thus resulting in a strong interaction. Amino acids contain amine, carboxylate, and occasionally thiol groups; therefore, many amino acids (28) and short peptide chains (29) can be detected via SERS. DNA bases can be detected with great sensitivity using aggregation of citrate-capped AgNPs (30), although $MgSO_4$, instead of the more common NaBr and NaCl, was used in this particular case because of its higher charge and lower affinity for the metal surfaces. More recently, the high surface affinity of iodide toward Ag was used to both clean and aggregate the AgNP surface, thereby enabling a robust detection of DNA bases (31). Advantageously, this study obtained signal from the phosphate backbone of DNA strands and identified the ratio of DNA bases present. These case studies illustrate the importance of the aggregating agent, particularly in the detection of charged analytes. Other examples of SAS include detection of pharmaceuticals/controlled substances (32–34) and highly polarizable dye molecules (19, 35–37). Quantification, however, is often problematic because uncontrolled aggregation causes variations in the local SERS enhancement. One solution is to substitute the NPs with SERS-active core-molecule-shell NPs where the outer shell captures the target molecules while the molecules trapped between the core and the shell act as internal standards, thereby offsetting the bias caused by the differences in the local enhancement factors (**Figure 2*a***) (38–40).

Although the aforementioned examples rely on the strong interaction between the analytes and NPs in solution, it is also possible to obtain SERS signal from molecules with a weak surface affinity using a "drop and dry" method. In this procedure, a small amount of the sample solution is dropped onto a SERS-active substrate and allowed to dry. The advantage of this method is twofold: The analyte is concentrated during the drying process, and removal of the solvent promotes physisorption of the analyte. Unfortunately, the success of this method depends strongly on the nature of the SERS substrate. For example, the detection of uranyl and neptunyl ions (UO_2^{2+} and NpO_2^{2}) was improved by several orders of magnitude when aqueous solutions of actinyl ions were dried onto silver doped sol-gel films instead of substrates prepared by evaporating silver onto silica NPs (41). Alternatively, if the analyte is already concentrated at a specific location, such as on a thin-layer chromatography plate (42) or a piece of contaminated farm produce (43), or there is forensic evidence of the inks on forged documents (44), drop-drying NPs at the location of the analyte can give rise to SERS signal. For instance, after the separation of a mixture of substituted aromatic water pollutants using thin-layer chromatography, AgNPs were dropped and dried directly onto the separated spots. SERS spectra recorded at those spots were then used to identify individual compounds (42).

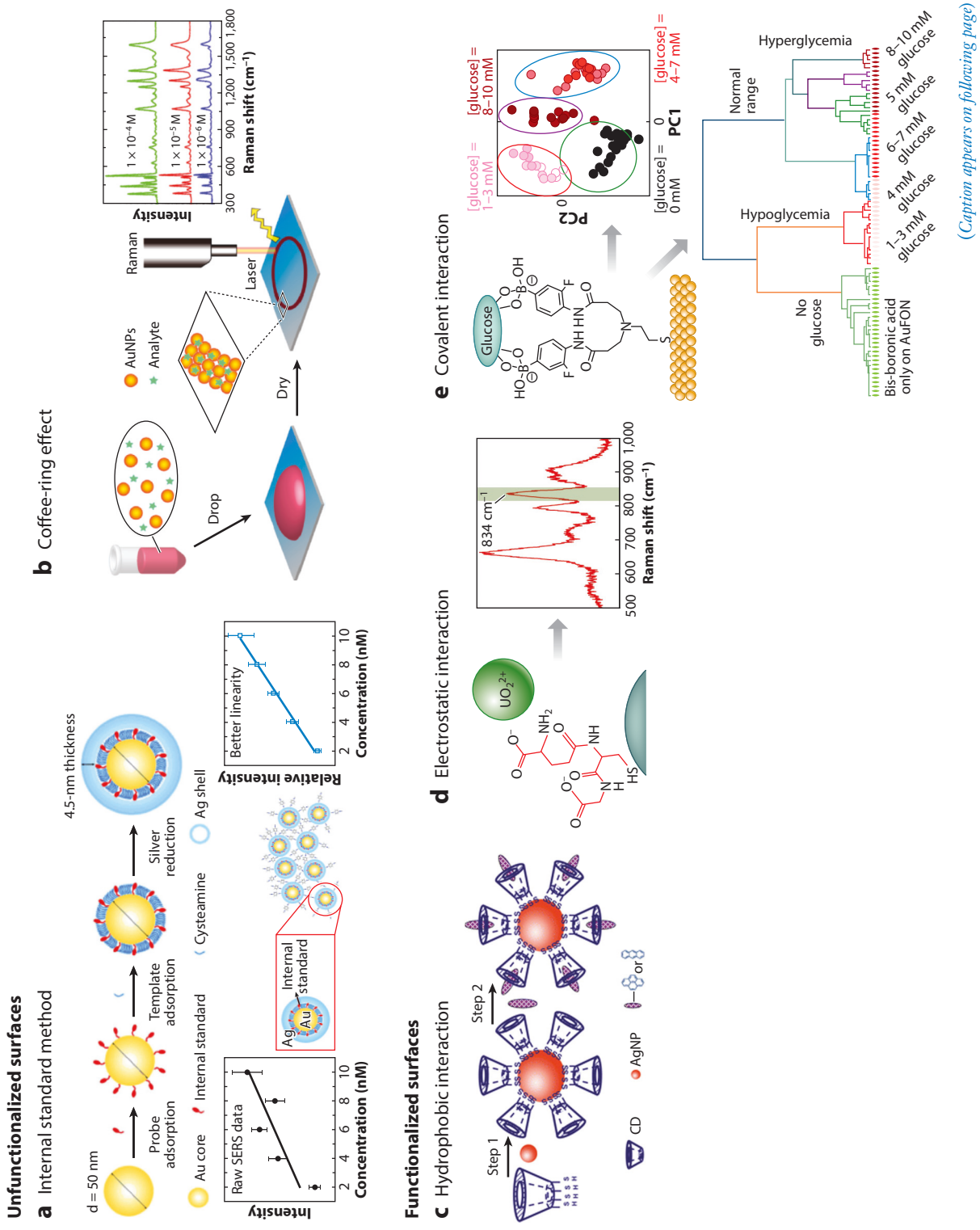

(Caption appears on following page)

Figure 2 (*Figure appears on preceding page*)

Surface-affinity strategies. (*a*) With the internal standard method, quantitative analysis of SERS data is improved by trapping internal standard molecules between an AuNP and a silver shell, leaving an unfunctionalized silver surface for the capture of analyte. Panel adapted with permission from Reference 38. Copyright 2015, John Wiley and Sons. (*b*) The coffee-ring effect occurs when PAHs are detected using the enhancement gained from a coffee ring of analyte and nanoparticles, formed by dropping and drying a nanoparticle-analyte solution on a silicon wafer. Panel adapted with permission from Reference 47. Copyright 2014, American Chemical Society. (*c*) In hydrophobic interaction, hydrophobic pockets created by functionalizing an AgNP with cyclodextrin lead to sensitive detection of nonpolar molecules, such as PAHs. Panel adapted with permission from Reference 59. Copyright 2010, Royal Society of Chemistry. (*d*) Electrostatic interaction between a negative carboxylate and a positive uranyl ion (UO_2^{2+}) affords sensitive detection of uranium in solution. Panel adapted with permission from Reference 60. Copyright 2017, Royal Society of Chemistry. (*e*) Covalent bonds formed between glucose and boronic acid groups lead to sensitive detection of glucose. Data processing using PC analysis combined with hierarchical cluster analysis effectively identifies healthy or unhealthy blood sugar levels. Panel adapted with permission from Reference 69. Copyright 2016, American Chemical Society. Abbreviations: AgNP, silver nanoparticle; AuFON, gold film over nanosphere; AuNP, gold nanoparticle; CD, cyclodextrin; CMS, colloidal mesoporous silica; PAH, polycyclic aromatic hydrocarbon; PC, principal component; SERS, surface-enhanced Raman spectroscopy.

The drop and dry procedure can be extended by adding SERS-active NPs into the sample solution and subsequently dropping the mixture onto a surface. As the solution evaporates, the NPs and analytes tend to concentrate and form a ring structure on the surface, known as the "coffee-ring effect" (45), which results in higher concentrations of the analytes and a greater density of hotspots in the ring region. Taking advantage of this effect, the detection of malachite green and arsenic in water (46), polycyclic aromatic hydrocarbons (PAHs) in water and methanol (**Figure 2*b***) (47), and the pesticide thiram on apple peels (48) was achieved with excellent sensitivity. Interestingly, evaporating a drop of AgNP solution onto a fluorosilylated silicon wafer can greatly weaken the coffee ring effect, resulting in a more densely packed assembly of NPs (49). When doing this, the most intense signal was observed at an intermediate point between the wet state and the dry state. This phenomenon was attributed to the formation of a three-dimensional (3D) hotspot matrix with minimal polydispersity of particle size and maximal uniformity of interparticle distance during the evaporation process. Using the 3D-hotspot matrix method, various nondye analytes can be detected in femtomolar concentrations with excellent reproducibility (50).

The ability to infer the orientation of the molecule on the nanostructure is an additional benefit of direct adsorption of the analyte to the surface. For example, early SERS studies of amino acids and nucleotides explained in detail how the relative intensities of specific bands indicate interaction of different functional groups with the surface (51). More recently, the orientation of chalcogen dyes and rhodamine 6G have been explored (52, 53).

2.2. Functionalized Substrates

Unfunctionalized surfaces are susceptible to interferences from nonspecific interactions. This is a critical disadvantage, and can be quite problematic, for samples with complex matrices. To combat the lack of selectivity, many groups have turned to nanostructures functionalized with a broad variety of receptor molecules, which then present a specificity to the molecule of interest. Though this scheme sounds promising given the large library of known receptors, the choice of the receptor molecule is limited by two factors: the size of the receptor molecule and the Raman cross section of the receptor molecules relative to the analytes. If the receptor molecules are bulky, as is the case with antibodies, the captured molecules may still be too far from the surface to experience strong enhancement. The first-layer effect, where the receptor molecules experience more enhancement than the more remote analytes, further suggests that the Raman cross section of the analyte should be greater than that of the first-layer molecules to promote signal from the analyte over the receptors. Generally speaking, the receptor molecules should be small (<2 nm)

and have small Raman cross sections relative to the analyte. Practically, it is difficult to utilize receptors that contain highly polarizable aromatic structures.

The use of alkanethiols to form a partition layer is another potential strategy, as it allows molecules to partition into the layer, thereby bringing the analyte closer to the surface resulting in a higher SERS signal. Van Duyne and coworkers (54) demonstrated the continuous monitoring of glucose in a mouse model using decanethiol as a partition layer with clinically relevant concentrations. Similarly, detection of other molecules such as polychlorinated biphenyls (PCBs) and PAHs have been reported using a partition layer scheme (55, 56). Cyclodextrin-modified surfaces, similar to alkanethiol partition layers, contain hydrophobic pockets and have also been used for sensitive detection of PCBs (57), pesticides (58), and PAHs (**Figure 2*c***) (59). A major disadvantage of schemes based on the partition layer effect is their lack of selectivity, which often necessitates an additional receptor–analyte interaction to enhance the specificity.

Electrostatic interactions can also increase the affinity of an analyte to substrate. For example, negatively charged surfaces, usually created by functionalizing the surface with carboxylate or phosphonate groups, demonstrate affinity for oxocations (60–63). Uranyl, for example, was selectively detected at low concentrations, relying on the attraction of the positive uranyl ion to the negative carboxylates of glutathione (**Figure 2*d***) (60). Similarly, positively charged surfaces, typically created by functionalizing the surface with amine groups, demonstrate affinity for oxyanions and result in successful detection of perchlorate, nitrate, and sulfate (64, 65). DNA detection with single-nucleobase modification sensitivity has also been accomplished utilizing spermine-functionalized NPs (66). More detailed information on SERS-based detection of small inorganic molecules, including oxyanions and cations, was recently reviewed by Alvarez-Puebla & Liz-Marzan (67).

Covalent interaction between the analyte and a functionalized surface is another useful way to deliver detection of targeted analytes. He and coworkers (68) detected and discriminated bacteria based on the covalent interaction between the receptor, 4-mercaptophenylboronic acid (4-MPBA,) and the glyco-sites on the cell wall of the bacteria. The boronic acid–diol interaction has also been applied in the successful detection of glucose with detection limits in clinically relevant concentrations (**Figure 2*e***) (69). TNT can be detected using the reaction between cysteine and TNT, which results in the formation of the Meisenheimer complex (70).

Given the complex and often unpredictable nature of SERS signals in the presence of interferences, and that the analyte signal can be weak relative to the interferences, multivariate analysis may be employed to mine the data for more reliable quantification and classification. To this end, a variety of statistical analysis procedures are commonly applied to complicated data sets. Some examples include principal component analysis (PCA) and support vector machines (SVMs), which are good methods for categorizing data and often used in combination with hierarchical cluster analysis (HCA) to cluster data. Partial least squares regression (PLSR) has also been frequently used to improve quantification. PCA has been utilized for the successful detection and discrimination of bacteria such as *Escherichia coli* and salmonella, and biomolecules such as influenza nucleoproteins (71, 72). SERS with data analysis by PCA HCA (69) was successfully used to identify and categorize hypoglycemic, normal, and hyperglycemic samples (**Figure 2*e***). Separately, similar analysis was used to identify healthy and cancerous cells (73). The SVM (74) has also been used for discrimination of healthy or cancerous cells and markers, whereas the PLSR model has improved quantitative detection of cancer markers (75).

3. SERS-TAG STRATEGIES

STSs rely on the signal from a Raman reporter attached to the NP, rather than using the intrinsic Raman response from the analyte itself. This approach circumvents the often difficult task of bringing the analyte into close proximity with the substrate. Specificity is achieved by attaching

an analyte-selective targeting ligand such as an antibody, aptamer, small molecule, or molecular-imprinted polymer (76–81) to the SERS-tagged NP. When exposed to the analyte, several changes can be monitored: (*a*) immobilization or accumulation of the SERS-tags at specific locations; (*b*) clustering or declustering of the SERS-tags, which results in generation or elimination of hotspots; and (*c*) reduced or increased distance between the Raman reporter and the SERS-active substrate.

3.1. SERS-Tag Immobilization

In the case of location-specific accumulation, the SERS-tags function as molecular beacons; however, they offer better photostability and multiplexing potential than their fluorescent analogs (20, 21). If the analytes are prelocated or captured on a specific stationary phase, for example, in an enzyme-linked immunosorbent assay (ELISA), the SERS-tag binding reveals the position and concentration of the analyte. To date, this method is one of the most successful and universal applications of SERS, finding utility ranging from cancer imaging and immunoassays to barcoding. Multiple recent reviews (76–78, 82) discuss these exciting applications.

Two recent advances in this area are notable. The first of these improves both the magnitude and homogeneity of the enhancement factor via the development of plasmonic intrananogap NPs (83, 84). In particular, Raman dyes confined in well-controlled intrananogaps (1 nm or smaller) generate dramatic and reproducible SERS signal due to the plasmon coupling within the uniform gap. As a result, those NPs generate robust and reproducible single particle–level SERS and were used for bioimaging with a wide-field excitation Raman setup (85). The second advance addresses false positives arising from nonspecific binding even in the presence of a SERS-tag tailored to the target. Oseledchyk et al. (86) demonstrated that a ratiometric approach enabled detection of tumors as small as 370 μm in a murine model of human ovarian adenocarcinoma (**Figure 3*a***). Specifically, an antifolate receptor–modified SERS-tag targeted the tumors, whereas nontargeted SERS-tags accounted for the nonspecific adherence. Therefore, the ratio of the signal between targeted and nontargeted tags in the tumor lesions reflects the location of the tumors while minimizing the false-positive results. A similar ratiometric strategy has also been applied to reduce the false-positive signals in immunoassays (87).

3.2. Hotspot Modulation

In the second STS case, the SERS signal is modulated by creating or dispersing regions of increased electromagnetic enhancement, known as hotspots (88). Electromagnetic hotspots are found at the junctions between NPs (89, 90), and depending upon the substrate, reporter molecule and gap-size hotspots can provide SERS enhancements of 5–8 orders of magnitude (91–93). Importantly for this scheme, the EF is strongly modulated by nanometer changes in the gap size. Utilizing this impressive enhancement, a "turn-on" or "turn-off" method can be designed based on the creation or elimination of hotspots due to the presence of analytes.

For the turn-on method, the creation of hotspots increases SERS signal from a Raman reporter. These hotspots are generated from NPs functionalized with ligands that selectively bind to the analyte at two different sites. As a result, the NP is brought into close proximity to a plasmonic substrate or another NP and generates a dramatic increase in SERS signal from the Raman reporters (94, 95). For example, Li et al. (96) detected As^{3+} with a limit of detection (LOD) of 0.76 ppb using Ag NPs functionalized with glutathione capture ligands and 4-mercaptopyridine (4-MPY) Raman reporters. The glutathione ligands selectively capture As^{3+} ions, creating a link between AgNPs and simultaneously generating a signal from the Raman reporter 4-MPY. Coupling this scheme

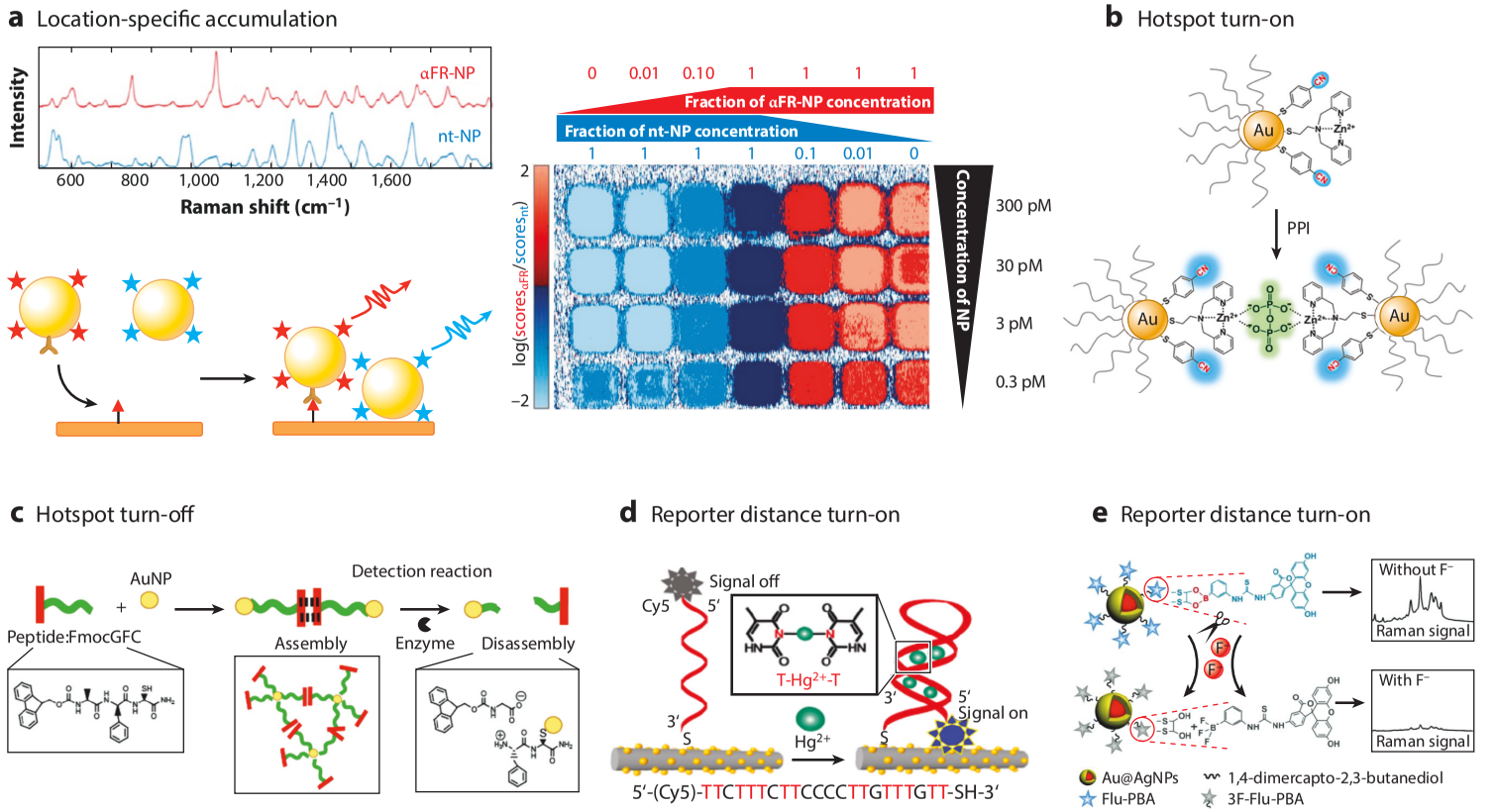

Figure 3

SERS-tag strategies. (*a*) Location-specific accumulation: The ratio of nonspecific binding agent (nt-NP) versus specific binding agent (αFR-NP). A high fraction of the red binding agent indicates antifolate receptor binding. Panel adapted with permission from Reference 86. Copyright 2017, American Chemical Society. (*b*) Hotspot turn-on: The strong nitrile signal in the SERS silent region indicates binding of PPI to the DPA-Zn^{2+} complex. Panel adapted with permission from Reference 97. Copyright 2017, American Chemical Society. (*c*) Hotspot turn-off: The enzyme cleaves the peptide-FMOC linker, resulting in a disaggregation of NPs and a turn-off of the SERS signal. Panel adapted with permission from Reference 105. Copyright 2010, American Chemical Society. (*d*) Reporter distance turn-on: A turn-on scheme where Hg^{2+} ions cause the DNA probe to fold, bringing the NP and substrate into contact. Panel adapted with permission from Reference 109. Copyright 2015, American Chemical Society. (*e*) Reporter distance turn-off: Fluoride ions release the Raman-active fluorescein boronic acid dye from the NP surface, resulting in detection of a SERS turn-off. Panel adapted with permission from Reference 114. Copyright 2017, Royal Society of Chemistry. Abbreviations: AgNP, silver nanoparticle; AuNP, gold nanoparticle; Cy5, cyanine 5; FMOC, *N*-(fluorenyl-9-methoxycarbonyl); NP, nanoparticle; PBA, phenylboronic acid; PPI, pyrophosphate; SERS, surface-enhanced Raman spectroscopy.

with reporters that exhibit a strong response in the silent region yields a background-free method for in situ imaging of pyrophosphate (**Figure 3*b***) (97). In particular, AuNPs were functionalized with bis(2-pyridylmethyl)amine (DPA)-Zn^{2+} complex, which strongly binds to the pyrophosphate at two sites, creating an NP dimer. To indicate binding, 4-mercaptobenzonitrile Raman reporters provide the silent region response due to the nitrile stretch. Similarly, this method has been applied to detection of Cu^{2+} (98), Cd^{2+} (99), protein (100), DNA, and RNA (101–104).

For the turn-off method, the analyte disrupts the link between the plasmonic substrates and consequently eliminates the preexisting hotspots, lowering the SERS signal from the Raman reporter. In a report by Maher et al. (105), the NP dimer-linking ligands, consisting of *N*-(fluorenyl-9-methoxycarbonyl) (FMOC) groups terminated with peptides, have an inherent SERS signal. When an enzyme with particular peptide selectivity is introduced, it cleaves the peptide–FMOC sequence, causing disaggregation, thus lowering the overall SERS signal (**Figure 3*c***). Akin to ligand cleavage, electrostatic interactions can disrupt aggregations. For detection of the medication heparin, Zhang et al. (106) aggregated AuNPs by interaction of protamine and Raman reporter 4-mercaptobenzoic acid (4-MBA). Heparin has a preferential electrostatic affinity for protamine, breaking up the aggregation and causing a significant decrease in the SERS intensity. This electrostatic interaction method has also been applied for enzymatic detection of thrombin with the arginine peptide (107). The turn-off method can also be applied to detection of Pb^{2+}, as demonstrated by Wang & Irudayaraj (108), who used thiol-functionalized DNAzymes along with 4-MBA reporters to create hotspots. Pb^{2+} cleaves a strand of DNAzyme, destroying the hotspot and permitting a 20-nM LOD.

3.3. Distance Modulation

In a variation on the previously discussed aggregation-based schemes, the final case of STS modulates the signal by changing the distance between the Raman reporters and the substrate. In this method, resonant dyes are typically linked to one end of an analyte-responsive ligand (e.g., DNAzyme, DNA, or RNA) while the other end of the ligand is loaded onto a SERS substrate. Introduction of the analyte induces a change in the ligand, which brings the Raman reporters closer or further from the substrate and results in a turn-on or turn-off signal.

For the turn-on scheme, dye molecules are generally located at the far end of the ligand, and the ligand will be bent upon interaction with the analytes, bringing the Raman reporters closer to the substrate. He and coworkers (109) reported Hg^{2+} detection using a cyanine 5 (Cy5)-labeled thymine (T)-rich single-stranded DNA (ssDNA) probe (**Figure 3*d***). In the presence of Hg^{2+}, the linear structure of ssDNA assembled on the substrate turned into a hairpin structure through the formation of T-Hg^{2+}-T. Consequently, the Cy5 was brought close to the surface, producing a strong Cy5 response. They also showed reversibility by adding iodide, a chelating agent for Hg^{2+}, to restore the ssDNA to linear form. In a following study, Pb^{2+} was detected using a Pb^{2+}-cleavable DNAzyme (110). The turn-on strategy has additionally been applied to detection of adenosine 5′-triphosphate (ATP), cocaine, and nucleic acids (111–113).

For the turn-off scheme, dye molecules begin close to the substrate, and the subsequent interaction with the analyte will either change the conformation of the ligand, thereby resulting in increased separation between the Raman probe and the substrate, or cleave the bond between Raman reporter and the ligand, releasing the dye molecules. For example, Zhang et al. (114) introduced a method for sensitive detection of F^- based on a fluoride-induced cleavage reaction (**Figure 3*e***). They first functionalized NPs with diols and conjugated the fluorescein boronic acid to the NP through boronic acid–diol reaction. The presence of F^- cleaves the boronate ester and consequently releases the loaded dye, resulting in a decreased SERS response. Kim et al. (115)

detected the *BIGH3* gene, which is a biomarker for Avellino corneal dystrophy, by displacing a Cy5-labeled ssDNA that is bound to its complementary ssDNA anchored on the SERS substrate. Therefore, a drop in SERS signal was observed, indicating detection of the gene. For the turn-off method, the reporter signal decrease is often hard to discern at low concentrations compared to a clear presence of signal in the turn-on method. Therefore, the turn-off strategy has not been widely applied in SERS studies.

4. PROBE-MEDIATED STRATEGIES

Similar to the previously discussed STSs, PMSs measure Raman signal from the probe molecules instead of the analytes. Unlike STS, where the Raman reporter is unchanged in the presence of analyte, PMS relies on a specific reaction or interaction between the probe and analyte, which results in a changing SERS spectrum of the probe molecule. Three important questions should be considered when designing PMS SERS-based sensors: (*a*) Is this reaction or interaction creating a new absorption band close to the laser wavelength? (*b*) Is this reaction or interaction able to change the distance between the probe molecule and the SERS substrate? (*c*) Is the chemical or conformational change of the probe molecule after interaction with the analyte significant enough to appear in the SERS spectra?

4.1. Creating Resonance Raman Enhancement

The resonance Raman effect arises when the excitation wavelength closely matches the frequency of a molecular electronic transition. Fully harnessing this effect can result in very large (up to 10^6) enhancements in the Raman signal (116). Therefore, the signal from the newly formed resonant molecules obtained from reaction of the probe and the analyte stand out compared to nonresonant interferences even when the analyte is in low abundance compared to interferences. Interestingly, colorimetric assays and ELISAs rely on this same strategy and are widely used in laboratory and clinical settings. Because of their extreme sensitivity, SERS-based sensors employing PMS can be considered as alternatives to both ELISA and colorimetric methods, especially when the analyte is low in concentration.

Qu et al. (117), for example, reported a method for detection of formaldehyde by taking advantage of the Hantzsch reaction, which involves the cyclization of acetylacetone, formaldehyde, and ammonia to form DDL, a compound with a strong absorption at 415 nm (**Figure 4*a***). Under 457-nm laser excitation, surface-enhanced resonance Raman spectroscopy (SERRS) signal was obtained, resulting in an LOD of 10^{-11} M and superb selectivity over other aldehydes and ketones. Detection of formaldehyde was also achieved using a similar strategy but different probe molecules (118, 119). Correa-Duarte et al. (120) developed a nitrite sensor utilizing the Griess reaction to generate hotspots. They modified two batches of AgNPs with 4-aminobenzenethiol and 1-naphthylamine, respectively, then mixed them afterward. In the presence of the nitrite, 4-aminobenzenethiol and 1-naphthylamine generated a diazonium derivative with a broad absorption of approximately 512 nm, and this compound also pulls the NPs together to form hotspots. They demonstrated an LOD of 4×10^{-13} M for nitrite and also detected nitrate by using a cadmium pellet to reduce nitrate to nitrite. Laing et al. (121) showed that a 50-times lower LOD in detection of a tumor necrosis factor could be achieved by using SERRS instead of conventional colorimetric detection in a commercial ELISA kit. The PMS approach has been applied to analytes, including dopamine (122), hormones (123), proteins (124), and sulfide and methanol (125), and in each case, several orders of magnitude lower limits of detection compared to conventional colorimetric assays were obtained.

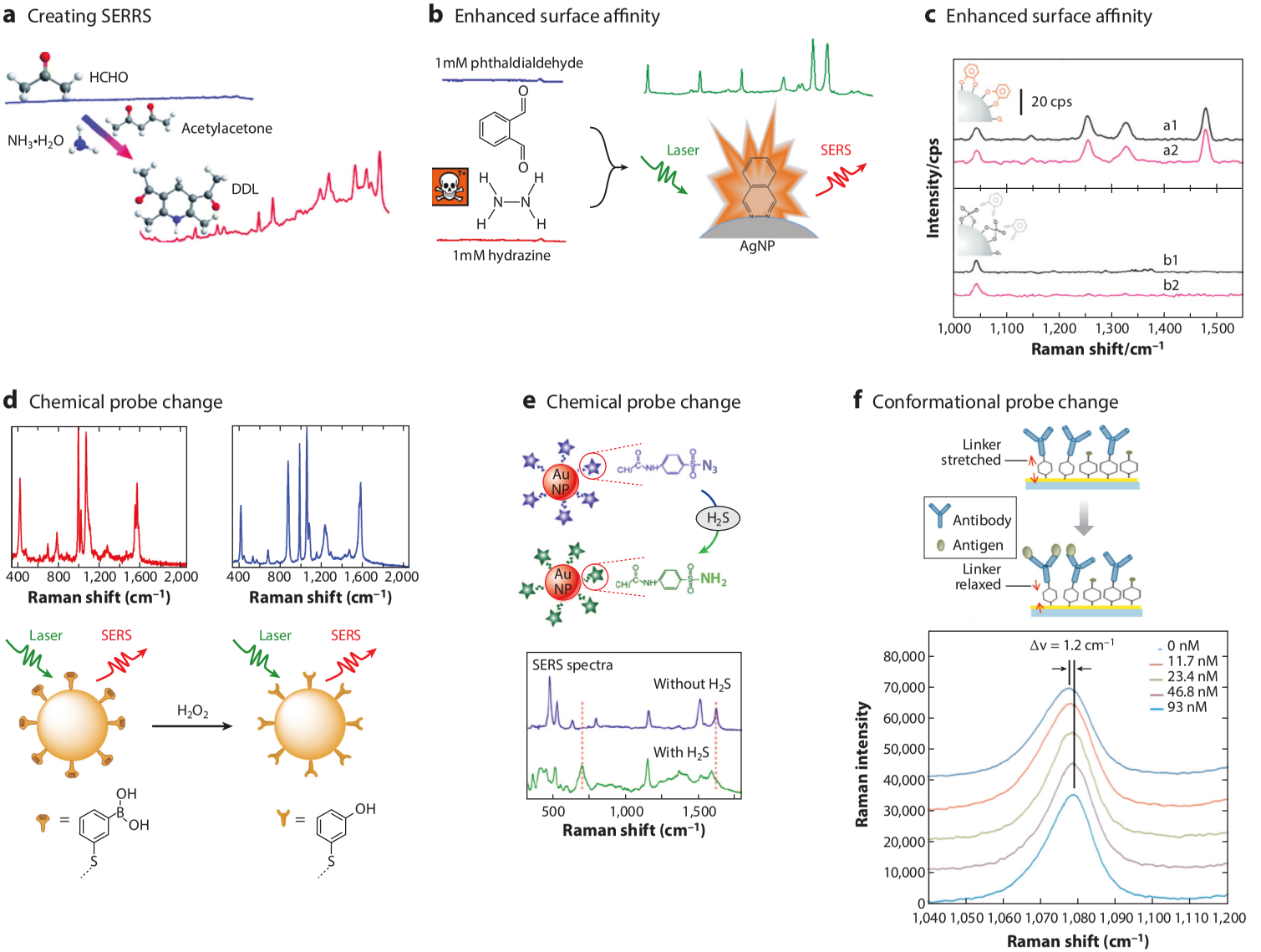

(Caption appears on following page)

Figure 4 (*Figure appears on preceding page*)

Probe-mediated strategies. (*a*) Creating SERRS: Before and after SERS spectra of formaldehyde and the DDL marker. Panel adapted with permission from Reference 117. Copyright 2012, Royal Society of Chemistry. (*b*) Enhanced surface affinity: Scheme of hydrazine reaction with a phthaldialdehyde probe to create the SERS-active phthalazine. Panel adapted with permission from Reference 126. Copyright 2015, American Chemical Society. (*c*) Probe replacement: Phosphate presence is indicated by a decrease in pyrocatechol SERS signal. Panel adapted with permission from Reference 128. Copyright 2015, Royal Society of Chemistry. (*d*) Chemical probe change: Scheme of the detection of H_2O_2 through selective oxidation of 3-MPBA to 3-HTTP. Panel adapted with permission from Reference 140. Copyright 2016, American Chemical Society. (*e*) Chemical probe change: Detection of H_2S through the 4-AA probe. Panel adapted with permission from Reference 144. Copyright 2015, John Wiley and Sons. (*f*) Conformational probe change: Mechanical stress of the Raman reporter and SERS peak shifts relative to anti-H1/4-ATP concentration changes. Panel adapted with permission from Reference 156. Copyright 2012, Royal Society of Chemistry. Abbreviations: 3-MPBA, 3-mercaptophenylboronic acid; 4-AA, 4-acetamidobenzenesulfonyl azide; ATP, adenosine 5′-triphosphate; SERS, surface-enhanced Raman spectroscopy; SERRS, surface-enhanced resonance Raman spectroscopy.

4.2. Surface-Affinity Modulation

As SERS is a highly surface distance–dependent method, the distance between the molecule and substrate largely determines the magnitude of the signal obtained. When designing methods utilizing this feature, two subcategories can be considered: creation of a turn-on signal when the analyte closes the distance between the probe and substrate and creation of a turn-off signal when analyte increases the distance between the probe and substrate. To diminish the distance, the analyte creates a surfacephilic functional group upon reaction with the probe. In both cases, the Raman probe is brought closer to the substrate. Gu & Camden (126) developed a hydrazine sensor based on the specific reaction between hydrazine and phthaldialdehyde (**Figure 4*b***). This reaction yields phthalazine, a molecule with a larger Raman cross section and better affinity to the SERS substrate due to the azo functionality. Zhang and coworkers (127) utilized the Ehrlich reaction to determine the concentration of indole-like hormones in plants with nanomolar sensitivity. The reaction between the probe p-(dimethylamino)benzaldehyde and the indole forms a cation, which has a strong absorption and induces aggregation in the AuNPs. This approach, therefore, benefits from both resonance Raman and hotspot enhancement. In the turn-off approach, the analyte can either displace the probe from the substrate or interact with the probe, generating a product with negligible surface affinity. For example, Ji et al. (128) reported a method to detect phosphate based on the displacement of catechols on a TiO_2 substrate (**Figure 4*c***). Also, utilizing the strong chelating nature of Hg^{2+}, Raman probes that originally attached on the SERS substrates are instead bound to Hg^{2+}, generating a complex with little affinity to the substrate (129–132). On the basis of the turn-off scheme, sensors have been designed to detect Cr^{6+} (133), H_2O_2, and glucose (134).

4.3. Reaction- or Interaction-Induced Spectral Change

Lastly, SERS is a very sensitive tool for probing the chemical and conformational changes of surface-bound molecules (135). Therefore, analytes that induce chemical or conformational changes in the surface-bound probe molecules can be readily detected via spectral change. It is often the case that several vibrational bands of the probe are unperturbed by the reaction. Advantageously, these unchanged bands serve as internal standards for robust quantification regardless of the variation in field enhancement caused by differences in the local substrate morphology. One of the earliest and most widely used applications of a chemical change–assisted method is monitoring the local pH in cells. pH-responsive probes, such as 4-MBA (136, 137), p-aminobenzenethiol (138), and 4-MPY (139) can map the pH distribution at the cellular level. Reactive oxygen species

(ROS), such as the hypochlorite ion, hydrogen peroxide, singlet oxygen, and various oxygen-based radicals, represent another important class of small molecules that play essential roles in a wide range of biological processes and disease states. Gu et al. (140) developed a method by using the 3-mercaptophenylboronic acid (3-MPBA)–modified AuNPs to detect exogenous and endogenous H_2O_2 in living cells (**Figure 4*d***). The reaction between 3-MPBA and H_2O_2 yields 3-hydroxythiophenol, which is easily observed in the SERS. Reproducible quantification was achieved using a ratiometric method. They further demonstrated that the probe was capable of delivering detection of glucose in urine and serum accurately when coupled with glucose oxidase. The sensing of other ROS has also been achieved using 4-hydroxythiophenol–, dihydrorhodamine-123–, and cytochrome C–modified probes (141–143). Besides the interest in these methods use for detecting ROS, great attention has been devoted to sensing small-molecule messengers, such as CO, NO, H_2S, and formaldehyde inside the cells. Long and coworkers (144) introduced a method in which they utilized 4-acetamidobenzenesulfonyl azide (4-AA)–functionalized AuNPs for detection of endogenous H_2S in living cells (**Figure 4*e***). In the presence of H_2S, 4-AA was reduced to 4-acetamidobenzenesulfonyl amine, which gave rise to the appearance of a band at 709 cm^{-1}. The unchanged band at 1,161 cm^{-1} served as an internal standard, greatly improving the quantification. They further reported a technique for detection of carbon monoxide in living cells by using palladacycle-modified AuNPs (145). Similarly, aminobenzene analogs and purpald-modified AuNPs have been demonstrated for detection of nitric oxide and formaldehyde in vitro and the detection of gaseous aldehyde in situ, respectively (146–150). It is important to note that not all chemical changes in the probe are reported on equally by the SERS spectra. Based on the aforementioned examples, chemical changes to groups directly linked to the aromatic molecules tend to more strongly influence the polarizability of the probes; therefore, these changes are more easily detected.

It is not always necessary, or possible, to chemically change the probe. Instead, one can rely on conformational change-assisted detection, which comes in two varieties: cases in which the probe is conformationally changed by interaction with the analyte and those in which the probe is linked to a receptor that acts to induce a change in the SERS reporter upon receptor binding the analyte. In the first category, the analyte usually induces a significant structural change of the probe. Alvarez-Puebla and coworkers (151) reported amino-MQAE–modified SERS microbeads that were capable of delivering a picomolar LOD of chloride. This group further detected FtsZ protein from *E. coli* using ZipA protein–functionalized NPs (152). In both cases, the analyte significantly alters the original geometry of the probe molecule, thereby yielding an easily discernable spectral change. Using the same principle, small molecules and ions such as fructose, Co^{2+}, Zn^{2+}, Cd^{2+}, and Hg^{2+} have been detected (153–155). If the analyte does not exhibit a strong interaction with the probe molecule, the probe, which is usually a thiophenol analog, can instead be linked to a receptor. When the probe-linked receptor captures the analyte, it increases the mechanical stress applied on the probes; consequently, the thiophenol analogs deform, and the concomitant change in the frequency shifts signal binding. This strategy has mostly enjoyed success when detecting large molecules, such as DNA, RNA, peptides, proteins, antigens, or other macromolecules, as they can induce a large stress response in the probe. Olivo and coworkers (156) linked influenza-H1 antibody with 4-ATP via EDC/NHS reaction, and upon binding with the SERS substrate, they observed bands that shifted in quantitative correlation with concentration of influenza-H1 antigen (**Figure 4*f***). Multiplexibility was also demonstrated by detecting influenza-H1 and anti-p53 antigens simultaneously using an anti-H1/4-ATP and anti-p52/6-MP–modified substrate with detection sensitivity comparable to conventional immunoassay. Following this scheme, other groups have reported the detection of oncoproteins such as c-Jun (157), c-MYC (158), α-fetaprotein, and glypican 3 (159) in clinical samples with picomolar sensitivity.

5. CONCLUSION

The past 40 years have seen phenomenal improvements in our understanding of the SERS effect and its application to analytical problems. The continuous improvement in sensitivity, selectivity, and quantification of SERS-based sensors has been exciting to witness. As researchers push forward, the future of clinical and industrial translation seems bright, as rationally designed SERS methods are becoming a reality. In this review, we provide a comprehensive categorization of SERS-based sensors using three major categories: SAS, STS, and PMS. The simplicity of our scheme is achieved by considering the origin of the SERS signal in each case. Lastly, we hope that this review serves as a guide to readers, especially newcomers to SERS, by highlighting the key considerations and general misconceptions in constructing SERS-based sensors.

DISCLOSURE STATEMENT

The authors are not aware of any affiliations, memberships, funding, or financial holdings that might be perceived as affecting the objectivity of this review.

ACKNOWLEDGMENTS

This work is supported by Advanced Diagnostics and Therapeutics at the University of Notre Dame (X.G.) and the US National Science Foundation under grants CHE-1709881 (J.P.C., M.J.T.), CHE-1709566 (J.P.C., J.E.O.), and CHE-1641479 (J.P.C, X.G.).

LITERATURE CITED

1. Xu ML, Gao Y, Han XX, Zhao B. 2017. Detection of pesticide residues in food using surface-enhanced Raman spectroscopy: a review. *J. Agric. Food Chem.* 65:6719–26
2. Golightly RS, Doering WE, Natan MJ. 2009. Surface-enhanced Raman spectroscopy and homeland security: A perfect match? *ACS Nano* 3:2859–69
3. Jamieson LE, Asiala SM, Gracie K, Faulds K, Graham D. 2017. Bioanalytical measurements enabled by surface-enhanced Raman scattering (SERS) probes. *Annu. Rev. Anal. Chem.* 10:415–37
4. Granger JH, Schlotter NE, Crawford AC, Porter MD. 2016. Prospects for point-of-care pathogen diagnostics using surface-enhanced Raman scattering (SERS). *Chem. Soc. Rev.* 45:3865–82
5. Cialla-May D, Zheng XS, Weber K, Popp J. 2017. Recent progress in surface-enhanced Raman spectroscopy for biological and biomedical applications: from cells to clinics. *Chem. Soc. Rev.* 46:3945–61
6. Sun F, Galvan DD, Jain P, Yu QM. 2017. Multi-functional, thiophenol-based surface chemistry for surface-enhanced Raman spectroscopy. *Chem. Commun.* 53:4550–61
7. Fleischmann M, Hendra PJ, McQuillan AJ. 1974. Raman-spectra of pyridine adsorbed at a silver electrode. *Chem. Phys. Lett.* 26:163–66
8. Albrecht MG, Creighton JA. 1977. Anomalously intense Raman-spectra of pyridine at a silver electrode. *J. Am. Chem. Soc.* 99:5215–17
9. Jeanmaire DL, Van Duyne RP. 1977. Surface Raman spectroelectrochemistry. 1. Heterocyclic, aromatic, and aliphatic-amines adsorbed on anodized silver electrode. *J. Electroanal. Chem.* 84:1–20
10. Moskovits M. 1978. Surface roughness and the enhanced intensity of Raman scattering by molecules adsorbed on metals. *J. Chem. Phys.* 69:4159–61
11. Moskovits M. 1985. Surface-enhanced spectroscopy. *Rev. Mod. Phys.* 57:783–826
12. Ding SY, Yi J, Li JF, Ren B, Wu DY, et al. 2016. Nanostructure-based plasmon-enhanced Raman spectroscopy for surface analysis of materials. *Nat. Rev. Mater.* 1:16021
13. Wei H, Xu HX. 2013. Hot spots in different metal nanostructures for plasmon-enhanced Raman spectroscopy. *Nanoscale* 5:10794–805

14. Ling X, Huang SX, Deng SB, Mao NN, Kong J, et al. 2015. Lighting up the Raman signal of molecules in the vicinity of graphene related materials. *Acc. Chem. Res.* 48:1862–70
15. Kennedy BJ, Spaeth S, Dickey M, Carron KT. 1999. Determination of the distance dependence and experimental effects for modified SERS substrates based on self-assembled monolayers formed using alkanethiols. *J. Phys. Chem. B* 103:3640–46
16. Tripathi A, Emmons ED, Fountain AW 3rd, Guicheteau JA, Moskovits M, Christesen SD. 2015. Critical role of adsorption equilibria on the determination of surface-enhanced Raman enhancement. *ACS Nano* 9:584–93
17. Kneipp K, Kneipp H, Kneipp J. 2006. Surface-enhanced Raman scattering in local optical fields of silver and gold nanoaggregates—from single-molecule Raman spectroscopy to ultrasensitive probing in live cells. *Acc. Chem. Res.* 39:443–50
18. Nie SM, Emory SR. 1997. Probing single molecules and single nanoparticles by surface-enhanced Raman scattering. *Science* 275:1102–6
19. Kneipp K, Wang Y, Kneipp H, Perelman LT, Itzkan I, et al. 1997. Single molecule detection using surface-enhanced Raman scattering (SERS). *Phys. Rev. Lett.* 78:1667–70
20. Hennig S, Mönkemöller V, Böger C, Müller M, Huser T. 2015. Nanoparticles as nonfluorescent analogues of fluorophores for optical nanoscopy. *ACS Nano* 9:6196–205
21. Laing S, Gracie K, Faulds K. 2016. Multiplex *in vitro* detection using SERS. *Chem. Soc. Rev.* 45:1901–18
22. Rodriguez-Lorenzo L, Fabris L, Alvarez-Puebla RA. 2012. Multiplex optical sensing with surface-enhanced Raman scattering: a critical review. *Anal. Chim. Acta* 745:10–23
23. Lee PC, Meisel D. 1982. Adsorption and surface-enhanced Raman of dyes on silver and gold sols. *J. Phys. Chem.* 86:3391–95
24. Otto A. 1991. Surface-enhanced Raman-scattering of adsorbates. *J. Raman Spectrosc.* 22:743–52
25. Otto A, Lust M, Pucci A, Meyer G. 2007. "SERS active sites", facts, and open questions. *Can. J. Anal. Sci. Spectrosc.* 52:150–71
26. Senapati D, Dasary SSR, Singh AK, Senapati T, Yu H, Ray PC. 2011. A label-free gold-nanoparticle-based SERS assay for direct cyanide detection at the parts-per-trillion level. *Chemistry* 17:8445–51
27. Ulman A. 1996. Formation and structure of self-assembled monolayers. *Chem. Rev.* 96:1533–54
28. Zhong ZY, Patskovskyy S, Bouvrette P, Luong JHT, Gedanken A. 2004. The surface chemistry of Au colloids and their interactions with functional amino acids. *J. Phys. Chem. B* 108:4046–52
29. Huang GG, Han XX, Hossain MK, Ozaki Y. 2009. Development of a heat-induced surface-enhanced Raman scattering sensing method for rapid detection of glutathione in aqueous solutions. *Anal. Chem.* 81:5881–88
30. Bell SEJ, Sirimuthu NMS. 2006. Surface-enhanced Raman spectroscopy (SERS) for sub-micromolar detection of DNA/RNA mononucleotides. *J. Am. Chem. Soc.* 128:15580–81
31. Xu L-J, Lei Z-C, Li J, Zong C, Yang CJ, Ren B. 2015. Label-free surface-enhanced Raman spectroscopy detection of DNA with single-base sensitivity. *J. Am. Chem. Soc.* 137:5149–54
32. Saleh TA, Al-Shalalfeh MM, Onawole AT, Al-Saadi AA. 2017. Ultra-trace detection of methimazole by surface-enhanced Raman spectroscopy using gold substrate. *Vib. Spectrosc.* 90:96–103
33. Faulds K, Smith WE, Graham D, Lacey RJ. 2002. Assessment of silver and gold substrates for the detection of amphetamine sulfate by surface enhanced Raman scattering (SERS). *Analyst* 127:282–86
34. Li M, Wu H, Wu Y, Ying Y, Wen Y, et al. 2017. Heterostructured cube Au–Ag composites for rapid Raman detection of antibiotic ciprofloxacin. *J. Raman Spectrosc.* 48:525–29
35. Nie S, Emory SR. 1997. Probing single molecules and single nanoparticles by surface-enhanced Raman scattering. *Science* 275:1102–6
36. Lee S, Choi J, Chen L, Park B, Kyong JB, et al. 2007. Fast and sensitive trace analysis of malachite green using a surface-enhanced Raman microfluidic sensor. *Anal. Chim. Acta* 590:139–44
37. Tran CD. 1984. Subnanogram detection of dyes on filter paper by surface-enhanced Raman scattering spectrometry. *Anal. Chem.* 56:824–26
38. Shen W, Lin X, Jiang C, Li C, Lin H, et al. 2015. Reliable quantitative SERS analysis facilitated by core–shell nanoparticles with embedded internal standards. *Angew. Chem. Int. Ed.* 54:7308–12
39. Pinkhasova P, Puccio B, Chou TM, Sukhishvili S, Du H. 2012. Noble metal nanostructure both as a SERS nanotag and an analyte probe. *Chem. Commun.* 48:9750–52

40. Fales AM, Tuan VD. 2015. Silver embedded nanostars for SERS with internal reference (SENSIR). *J. Mater. Chem. C* 3:7319–24
41. Bao L, Mahurin SM, Haire RG, Dai S. 2003. Silver-doped sol–gel film as a surface-enhanced Raman scattering substrate for detection of uranyl and neptunyl ions. *Anal. Chem.* 75:6614–20
42. Li D, Qu L, Zhai W, Xue J, Fossey JS, Long Y. 2011. Facile on-site detection of substituted aromatic pollutants in water using thin layer chromatography combined with surface-enhanced Raman spectroscopy. *Environ. Sci. Technol.* 45:4046–52
43. Liu BH, Han GM, Zhang ZP, Liu RY, Jiang CL, et al. 2012. Shell thickness-dependent Raman enhancement for rapid identification and detection of pesticide residues at fruit peels. *Anal. Chem.* 84:255–61
44. Braz A, Lopez-Lopez M, Garcia-Ruiz C. 2013. Raman spectroscopy for forensic analysis of inks in questioned documents. *Forensic Sci. Int.* 232:206–12
45. Deegan RD, Bakajin O, Dupont TF, Huber G, Nagel SR, Witten TA. 1997. Capillary flow as the cause of ring stains from dried liquid drops. *Nature* 389:827–29
46. Wang W, Yin Y, Tan Z, Liu J. 2014. Coffee-ring effect-based simultaneous SERS substrate fabrication and analyte enrichment for trace analysis. *Nanoscale* 6:9588–93
47. Xu J, Du J, Jing C, Zhang Y, Cui J. 2014. Facile detection of polycyclic aromatic hydrocarbons by a surface-enhanced Raman scattering sensor based on the Au coffee ring effect. *ACS Appl. Mater. Interfaces* 6:6891–97
48. Yang J-K, Kang H, Lee H, Jo A, Jeong S, et al. 2014. Single-step and rapid growth of silver nanoshells as SERS-active nanostructures for label-free detection of pesticides. *ACS Appl. Mater. Interfaces* 6:12541–49
49. Liu HL, Yang ZL, Meng LY, Sun YD, Wang J, et al. 2014. Three-dimensional and time-ordered surface-enhanced Raman scattering hotspot matrix. *J. Am. Chem. Soc.* 136:5332–41
50. Yang LB, Li P, Liu HL, Tang XH, Liu JH. 2015. A dynamic surface enhanced Raman spectroscopy method for ultra-sensitive detection: from the wet state to the dry state. *Chem. Soc. Rev.* 44:2837–48
51. Suh JS, Moskovits M. 1986. Surface-enhanced Raman-spectroscopy of amino-acids and nucleotide bases adsorbed on silver. *J. Am. Chem. Soc.* 108:4711–18
52. Kearns H, Sengupta S, Sasselli IR, Bromley L, Faulds K, et al. 2016. Elucidation of the bonding of a near infrared dye to hollow gold nanospheres—a chalcogen tripod. *Chem. Sci.* 7:5160–70
53. Turley HK, Hu ZW, Jensen L, Camden JP. 2017. Surface-enhanced resonance hyper-Raman scattering elucidates the molecular orientation of rhodamine 6g on silver colloids. *J. Phys. Chem. Lett.* 8:1819–23
54. Ma K, Yuen JM, Shah NC, Walsh JT, Glucksberg MR, Van Duyne RP. 2011. In vivo, transcutaneous glucose sensing using surface-enhanced spatially offset Raman spectroscopy: multiple rats, improved hypoglycemic accuracy, low incident power, and continuous monitoring for greater than 17 days. *Anal. Chem.* 83:9146–52
55. Bantz KC, Haynes CL. 2009. Surface-enhanced Raman scattering detection and discrimination of polychlorinated biphenyls. *Vib. Spectrosc.* 50:29–35
56. Jones CL, Bantz KC, Haynes CL. 2009. Partition layer-modified substrates for reversible surface-enhanced Raman scattering detection of polycyclic aromatic hydrocarbons. *Anal. Bioanal. Chem.* 394:303–11
57. Lu Y, Yao G, Sun K, Huang Q. 2015. β-Cyclodextrin coated SiO_2@Au@Ag core-shell nanoparticles for SERS detection of PCBs. *Phys. Chem. Chem. Phys.* 17:21149–57
58. Strickland AD, Batt CA. 2009. Detection of carbendazim by surface-enhanced Raman scattering using cyclodextrin inclusion complexes on gold nanorods. *Anal. Chem.* 81:2895–903
59. Xie Y, Wang X, Han X, Xue X, Ji W, et al. 2010. Sensing of polycyclic aromatic hydrocarbons with cyclodextrin inclusion complexes on silver nanoparticles by surface-enhanced Raman scattering. *Analyst* 135:1389–94
60. Trujillo MJ, Jenkins DM, Bradshaw JA, Camden JP. 2017. Surface-enhanced Raman scattering of uranyl in aqueous samples: implications for nuclear forensics and groundwater testing. *Anal. Methods* 9:1575–79
61. Ruan C, Luo W, Wang W, Gu B. 2007. Surface-enhanced Raman spectroscopy for uranium detection and analysis in environmental samples. *Anal. Chim. Acta* 605:80–86
62. Teiten B, Burneau A. 1997. Detection and sorption study of dioxouranium(VI) ions on *N*-(2-mercaptopropionyl)glycine-modified silver colloid by surface-enhanced Raman scattering. *J. Raman Spectrosc.* 28:879–84

63. Lu G, Forbes TZ, Haes AJ. 2016. SERS detection of uranyl using functionalized gold nanostars promoted by nanoparticle shape and size. *Analyst* 141:5137–43
64. Ruan C, Wang W, Gu B. 2006. Surface-enhanced Raman scattering for perchlorate detection using cystamine-modified gold nanoparticles. *Anal. Chim. Acta* 567:114–20
65. Mosier-Boss PA, Lieberman SH. 2000. Detection of nitrate and sulfate anions by normal Raman spectroscopy and SERS of cationic-coated, silver substrates. *Appl. Spectrosc.* 54:1126–35
66. Morla-Folch J, Xie H, Gisbert-Quilis P, Gómez de-Pedro S, Pazos-Perez N, et al. 2015. Ultrasensitive direct quantification of nucleobase modifications in DNA by surface-enhanced Raman scattering: the case of cytosine. *Angew. Chem. Int. Ed.* 54:13650–54
67. Alvarez-Puebla RA, Liz-Marzan LM. 2012. SERS detection of small inorganic molecules and ions. *Angew. Chem. Int. Ed.* 51:11214–23
68. Wang HY, Zhou YF, Jiang XX, Sun B, Zhu Y, et al. 2015. Simultaneous capture, detection, and inactivation of bacteria as enabled by a surface-enhanced Raman scattering multifunctional chip. *Angew. Chem. Int. Ed.* 54:5132–36
69. Sharma B, Bugga P, Madison LR, Henry A-I, Blaber MG, et al. 2016. Bisboronic acids for selective, physiologically relevant direct glucose sensing with surface-enhanced Raman spectroscopy. *J. Am. Chem. Soc.* 138:13952–59
70. Dasary SSR, Singh AK, Senapati D, Yu HT, Ray PC. 2009. Gold nanoparticle based label-free SERS probe for ultrasensitive and selective detection of trinitrotoluene. *J. Am. Chem. Soc.* 131:13806–12
71. Negri P, Kage A, Nitsche A, Naumann D, Dluhy RA. 2011. Detection of viral nucleoprotein binding to anti-influenza aptamers via SERS. *Chem. Commun.* 47:8635–37
72. Wu X, Xu C, Tripp RA, Y-W Huang, Zhao Y. 2013. Detection and differentiation of foodborne pathogenic bacteria in mung bean sprouts using field deployable label-free SERS devices. *Analyst* 138:3005–12
73. Chen Y, Zhang Y, Pan F, Liu J, Wang K, et al. 2016. Breath analysis based on surface-enhanced Raman scattering sensors distinguishes early and advanced gastric cancer patients from healthy persons. *ACS Nano* 10:8169–79
74. Zhang Y, Ye X, Xu G, Jin X, Luan M, et al. 2016. Identification and distinction of non-small-cell lung cancer cells by intracellular SERS nanoprobes. *RSC Adv.* 6:5401–7
75. Li M, Kang JW, Sukumar S, Dasari RR, Barman I. 2015. Multiplexed detection of serological cancer markers with plasmon-enhanced Raman spectro-immunoassay. *Chem. Sci.* 6:3906–14
76. Wang ZY, Zong SF, Wu L, Zhu D, Cui YP. 2017. SERS-activated platforms for immunoassay: probes, encoding methods, and applications. *Chem. Rev.* 117:7910–63
77. Lane LA, Qian XM, Nie SM. 2015. SERS nanoparticles in medicine: from label-free detection to spectroscopic tagging. *Chem. Rev.* 115:10489–529
78. Wang YQ, Yan B, Chen LX. 2013. SERS tags: novel optical nanoprobes for bioanalysis. *Chem. Rev.* 113:1391–428
79. Yin DY, Wang SS, He YJ, Liu J, Zhou M, et al. 2015. Surface-enhanced Raman scattering imaging of cancer cells and tissues via sialic acid-imprinted nanotags. *Chem. Commun.* 51:17696–99
80. Ye J, Chen Y, Liu Z. 2014. A boronate affinity sandwich assay: an appealing alternative to immunoassays for the determination of glycoproteins. *Angew. Chem. Int. Ed.* 53:10386–89
81. Liu J, Yin DY, Wang SS, Chen HY, Liu Z. 2016. Probing low-copy-number proteins in a single living cell. *Angew. Chem. Int. Ed.* 55:13215–18
82. Harmsen S, Wall MA, Huang RM, Kircher MF. 2017. Cancer imaging using surface-enhanced resonance Raman scattering nanoparticles. *Nat. Protoc.* 12:1400–14
83. Lim DK, Jeon KS, Hwang JH, Kim H, Kwon S, et al. 2011. Highly uniform and reproducible surface-enhanced Raman scattering from DNA-tailorable nanoparticles with 1-nm interior gap. *Nat. Nanotechnol.* 6:452–60
84. Nam JM, Oh JW, Lee H, Suh YD. 2016. Plasmonic nanogap-enhanced Raman scattering with nanoparticles. *Acc. Chem. Res.* 49:2746–55
85. Lee JH, Oh JW, Nam SH, Cha YS, Kim GH, et al. 2016. Synthesis, optical properties, and multiplexed Raman bio-imaging of surface roughness-controlled nanobridged nanogap particles. *Small* 12:4726–34

86. Oseledchyk A, Andreou C, Wall MA, Kircher MF. 2017. Folate-targeted surface-enhanced resonance Raman scattering nanoprobe ratiometry for detection of microscopic ovarian cancer. *ACS Nano* 11:1488–97
87. Chuong TT, Pallaoro A, Chaves CA, Li Z, Lee J, et al. 2017. Dual-reporter SERS-based biomolecular assay with reduced false-positive signals. *PNAS* 114:9056–61
88. Qian XM, Nie SM. 2008. Single-molecule and single-nanoparticle SERS: from fundamental mechanisms to biomedical applications. *Chem. Soc. Rev.* 37:912–20
89. Michaels AM, Nirmal M, Brus LE. 1999. Surface enhanced Raman spectroscopy of individual rhodamine 6g molecules on large Ag nanocrystals. *J. Am. Chem. Soc.* 121:9932–39
90. Michaels AM, Jiang, Brus L. 2000. Ag nanocrystal junctions as the site for surface-enhanced Raman scattering of single rhodamine 6g molecules. *J. Phys. Chem. B* 104:11965–71
91. Etchegoin PG, Le Ru E. 2008. A perspective on single molecule SERS: current status and future challenges. *Phys. Chem. Chem. Phys.* 10:6079–89
92. Ru ECL, Etchegoin PG, Meyer M. 2006. Enhancement factor distribution around a single surface-enhanced Raman scattering hot spot and its relation to single molecule detection. *J. Chem. Phys.* 125:204701
93. Petryayeva E, Krull UJ. 2011. Localized surface plasmon resonance: nanostructures, bioassays and biosensing—a review. *Anal. Chim. Acta* 706:8–24
94. Takenaka T, Eda K, Mabuchi M, Fujiyoshi Y, Uyeda N. 1984. Surface enhanced Raman scattering by isomeric monobromopyridines adsorbed on gold and silver sol particles. *Bull. Inst. Chem. Res.* 62:219–32
95. Camden JP, Dieringer JA, Wang Y, Masiello DJ, Marks LD, et al. 2008. Probing the structure of single-molecule surface-enhanced Raman scattering hot spots. *J. Am. Chem. Soc.* 130:12616–17
96. Li J, Chen L, Lou T, Wang Y. 2011. Highly sensitive SERS detection of As^{3+} ions in aqueous media using glutathione functionalized silver nanoparticles. *ACS Appl. Mater. Interfaces* 3:3936–41
97. Li M, Li J, Di H, Liu H, Liu D. 2017. Live-cell pyrophosphate imaging by in situ hot-spot generation. *Anal. Chem.* 89:3532–37
98. Wang Y, Su Z, Wang L, Dong J, Xue J, et al. 2017. SERS assay for copper(II) ions based on dual hot-spot model coupling with MarR protein: new Cu^{2+}-specific biorecognition element. *Anal. Chem.* 89:6392–98
99. Dasary SSR, Jones YK, Barnes SL, Ray PC, Singh AK. 2016. Alizarin dye based ultrasensitive plasmonic SERS probe for trace level cadmium detection in drinking water. *Sens. Actuators B* 224:65–72
100. Yan J, Su S, He S, He Y, Zhao B, et al. 2012. Nano rolling-circle amplification for enhanced SERS hot spots in protein microarray analysis. *Anal. Chem.* 84:9139–45
101. Fabris L, Dante M, Braun G, Lee SJ, Reich NO, et al. 2007. A heterogeneous PNA-based SERS method for DNA detection. *J. Am. Chem. Soc.* 129:6086–87
102. Braun G, Lee SJ, Dante M, Nguyen T-Q, Moskovits M, Reich N. 2007. Surface-enhanced Raman spectroscopy for DNA detection by nanoparticle assembly onto smooth metal films. *J. Am. Chem. Soc.* 129:6378–79
103. Cao YC, Jin R, Mirkin CA. 2002. Nanoparticles with Raman spectroscopic fingerprints for DNA and RNA detection. *Science* 297:1536–40
104. Liu H, Li Q, Li M, Ma S, Liu D. 2017. In situ hot-spot assembly as a general strategy for probing single biomolecules. *Anal. Chem.* 89:4776–80
105. Maher RC, Maier SA, Cohen LF, Koh L, Laromaine A, et al. 2010. Exploiting SERS hot spots for disease-specific enzyme detection. *J. Phys. Chem. C* 114:7231–35
106. Zhang CM, Liang X, You TT, Yang N, Gao YK, Yin PG. 2017. An ultrasensitive "turn-off" SERS sensor for quantitatively detecting heparin based on 4-mercaptobenzoic acid functionalized gold nanoparticles. *Anal. Methods* 9:2517–22
107. Wu ZT, Liu YZ, Zhou XD, Shen AG, Hu JM. 2013. A "turn-off" SERS-based detection platform for ultrasensitive detection of thrombin based on enzymatic assays. *Biosens. Bioelectron.* 44:10–15
108. Wang Y, Irudayaraj J. 2011. A SERS DNAzyme biosensor for lead ion detection. *Chem. Commun.* 47:4394–96
109. Sun B, Jiang XX, Wang HY, Song B, Zhu Y, et al. 2015. Surface-enhancement Raman scattering sensing strategy for discriminating trace mercuric ion (II) from real water samples in sensitive, specific, recyclable, and reproducible manners. *Anal. Chem.* 87:1250–56

110. Shi Y, Wang HY, Jiang XX, Sun B, Song B, et al. 2016. Ultrasensitive, specific, recyclable, and reproducible detection of lead ions in real systems through a polyadenine-assisted, surface enhanced Raman scattering silicon chip. *Anal. Chem.* 88:3723–29
111. Wu Y, Xiao FB, Wu ZY, Yu RQ. 2017. Novel aptasensor platform based on ratiometric surface-enhanced Raman spectroscopy. *Anal. Chem.* 89:2852–58
112. Chen JW, Jiang JH, Gao X, Liu GK, Shen GL, Yu RQ. 2008. A new aptameric biosensor for cocaine based on surface-enhanced Raman scattering spectroscopy. *Chemistry* 14:8374–82
113. Li YY, Zhao QC, Wang YD, Man TT, Zhou L, et al. 2016. Ultrasensitive signal-on detection of nucleic acids with surface-enhanced Raman scattering and exonuclease III-assisted probe amplification. *Anal. Chem.* 88:11684–90
114. Zhang J, He LF, Chen PR, Tian C, Wang JP, et al. 2017. A silica-based SERS chip for rapid and ultrasensitive detection of fluoride ions triggered by a cyclic boronate ester cleavage reaction. *Nanoscale* 9:1599–606
115. Kim S, Jeong SN, Bae S, Chung H, Yoo SY. 2016. Sensitive surface enhanced Raman scattering-based detection of a *BIGH3* point mutation associated with Avellino corneal dystrophy. *Anal. Chem.* 88:11288–92
116. Efremov EV, Ariese F, Gooijer C. 2008. Achievements in resonance Raman spectroscopy review of a technique with a distinct analytical chemistry potential. *Anal. Chim. Acta* 606:119–34
117. Qu WG, Lu LQ, Lin L, Xu AW. 2012. A silver nanoparticle based surface enhanced resonance Raman scattering (SERRS) probe for the ultrasensitive and selective detection of formaldehyde. *Nanoscale* 4:7358–61
118. Zhang ZM, Zhao C, Ma YJ, Li GK. 2014. Rapid analysis of trace volatile formaldehyde in aquatic products by derivatization reaction-based surface enhanced Raman spectroscopy. *Analyst* 139:3614–21
119. Lv ZY, Mei LP, Chen WY, Feng JJ, Chen JY, Wang AJ. 2014. Shaped-controlled electrosynthesis of gold nanodendrites for highly selective and sensitive SERS detection of formaldehyde. *Sens. Actuators B* 201:92–99
120. Correa-Duarte MA, Perez NP, Guerrini L, Giannini V, Alvarez-Puebla RA. 2015. Boosting the quantitative inorganic surface-enhanced Raman scattering sensing to the limit: the case of nitrite/nitrate detection. *J. Phys. Chem. Lett.* 6:868–74
121. Laing S, Hernandez-Santana A, Sassmannshausen J, Asquith DL, McInnes IB, et al. 2011. Quantitative detection of human tumor necrosis factor α by a resonance Raman enzyme-linked immunosorbent assay. *Anal. Chem.* 83:297–302
122. Kayat M, Volkan M. 2012. New approach for the surface enhanced resonance Raman scattering (SERRS) detection of dopamine at picomolar (pM) levels in the presence of ascorbic acid. *Anal. Chem.* 84:7729–35
123. Sui HM, Wang Y, Zhang XL, Wang XL, Cheng WN, et al. 2016. Ultrasensitive detection of thyrotropin-releasing hormone based on azo coupling and surface-enhanced resonance Raman spectroscopy. *Analyst* 141:5181–88
124. Sloan-Dennison S, Laing S, Shand NC, Graham D, Faulds K. 2017. A novel nanozyme assay utilising the catalytic activity of silver nanoparticles and SERRS. *Analyst* 142:2484–90
125. Chen Z, Li G, Zhang Z. 2017. Miniaturized thermal-assisted purge-and-trap technique coupling with surface-enhanced Raman scattering for trace analysis of complex samples. *Anal. Chem.* 89:9593–600
126. Gu X, Camden JP. 2015. Surface-enhanced Raman spectroscopy-based approach for ultrasensitive and selective detection of hydrazine. *Anal. Chem.* 87:6460–64
127. Wang F, Gu X, Zheng C, Dong F, Zhang L, et al. 2017. Ehrlich reaction evoked multiple spectral resonances and gold nanoparticle hotspots for Raman detection of plant hormone. *Anal. Chem.* 89:8836–43
128. Ji W, Song W, Tanabe I, Wang Y, Zhao B, Ozaki YH. 2015. Semiconductor-enhanced Raman scattering for highly robust SERS sensing: the case of phosphate analysis. *Chem. Commun.* 51:7641–44
129. Grasseschi D, Zamarion VM, Araki K, Toma HE. 2010. Surface enhanced Raman scattering spot tests: a new insight on Feigl's analysis using gold nanoparticles. *Anal. Chem.* 82:9146–49
130. Du YX, Liu RY, Liu BH, Wang SH, Han MY, Zhang ZP. 2013. Surface-enhanced Raman scattering chip for femtomolar detection of mercuric ion (II) by ligand exchange. *Anal. Chem.* 85:3160–65

131. Ren W, Zhu CZ, Wang EK. 2012. Enhanced sensitivity of a direct SERS technique for Hg^{2+} detection based on the investigation of the interaction between silver nanoparticles and mercury ions. *Nanoscale* 4:5902–9
132. Senapati T, Senapati D, Singh AK, Fan Z, Kanchanapally R, Ray PC. 2011. Highly selective SERS probe for Hg(II) detection using tryptophan-protected popcorn shaped gold nanoparticles. *Chem. Commun.* 47:10326–28
133. Ji W, Wang Y, Tanabe I, Han XX, Zhao B, Ozaki Y. 2015. Semiconductor-driven "turn-off" surface-enhanced Raman scattering spectroscopy: application in selective determination of chromium(VI) in water. *Chem. Sci.* 6:342–48
134. Dong J, Guo GM, Xie W, Li Y, Zhang MY, Qian WP. 2015. Free radical-quenched SERS probes for detecting H_2O_2 and glucose. *Analyst* 140:2741–46
135. Gu X, Wang H, Camden JP. 2017. Utilizing light-triggered plasmon-driven catalysis reactions as a template for molecular delivery and release. *Chem. Sci.* 8:5902–8
136. Talley CE, Jusinski L, Hollars CW, Lane SM, Huser T. 2004. Intracellular pH sensors based on surface-enhanced Raman scattering. *Anal. Chem.* 76:7064–68
137. Kneipp J, Kneipp H, Wittig B, Kneipp K. 2007. One- and two-photon excited optical pH probing for cells using surface-enhanced Raman and hyper-Raman nanosensors. *Nano Lett.* 7:2819–23
138. Zong SF, Wang ZY, Yang J, Cui YP. 2011. Intracellular pH sensing using *p*-aminothiophenol functionalized gold nanorods with low cytotoxicity. *Anal. Chem.* 83:4178–83
139. Zheng XS, Hu P, Cui Y, Zong C, Feng JM, et al. 2014. BSA-coated nanoparticles for improved SERS-based intracellular pH sensing. *Anal. Chem.* 86:12250–57
140. Gu X, Wang H, Schultz ZD, Camden JP. 2016. Sensing glucose in urine and serum and hydrogen peroxide in living cells by use of a novel boronate nanoprobe based on surface-enhanced Raman spectroscopy. *Anal. Chem.* 88:7191–97
141. Wang WK, Zhang LM, Li L, Tian Y. 2016. A single nanoprobe for ratiometric imaging and biosensing of hypochlorite and glutathione in live cells using surface-enhanced Raman scattering. *Anal. Chem.* 88:9518–23
142. Jiang C, Liu R, Han G, Zhang Z. 2013. A chemically reactive Raman probe for ultrasensitively monitoring and imaging the *in vivo* generation of femtomolar oxidative species as induced by anti-tumor drugs in living cells. *Chem. Commun.* 49:6647–49
143. Qu LL, Li DW, Qin LX, Mu J, Fossey JS, Long YT. 2013. Selective and sensitive detection of intracellular $O_2^{\cdot-}$ using Au NPs/cytochrome *c* as SERS nanosensors. *Anal. Chem.* 85:9549–55
144. Li DW, Qu LL, Hu K, Long YT, Tian H. 2015. Monitoring of endogenous hydrogen sulfide in living cells using surface-enhanced Raman scattering. *Angew. Chem. Int. Ed.* 54:12758–61
145. Cao Y, Li DW, Zhao LJ, Liu XY, Cao XM, Long YT. 2015. Highly selective detection of carbon monoxide in living cells by palladacycle carbonylation-based surface enhanced Raman spectroscopy nanosensors. *Anal. Chem.* 87:9696–701
146. Gil PR, Vazquez-Vazquez C, Giannini V, Callao MP, Parak WJ, et al. 2013. Plasmonic nanoprobes for real-time optical monitoring of nitric oxide inside living cells. *Angew. Chem. Int. Ed.* 52:13694–98
147. Cui J, Hu K, Sun JJ, Qu LL, Li DW. 2016. SERS nanoprobes for the monitoring of endogenous nitric oxide in living cells. *Biosens. Bioelectron.* 85:324–30
148. Xu Q, Liu W, Li L, Zhou F, Zhou J, Tian Y. 2017. Ratiometric SERS imaging and selective biosensing of nitric oxide in live cells based on trisoctahedral gold nanostructures. *Chem. Commun.* 53:1880–83
149. Wang Y, Deng XH, Liu JW, Tang H, Jiang JH. 2013. Surface enhanced Raman scattering based sensitive detection of histone demethylase activity using a formaldehyde-selective reactive probe. *Chem. Commun.* 49:8489–91
150. Zhang Z, Yu W, Wang J, Luo D, Qiao X, et al. 2017. Ultrasensitive surface-enhanced Raman scattering sensor of gaseous aldehydes as biomarkers of lung cancer on dendritic Ag nanocrystals. *Anal. Chem.* 89:1416–20
151. Tsoutsi D, Montenegro JM, Dommershausen F, Koert U, Liz-Marzan LM, et al. 2011. Quantitative surface-enhanced Raman scattering ultradetection of atomic inorganic ions: the case of chloride. *ACS Nano* 5:7539–46

152. Ahijado-Guzmán R, Gómez-Puertas P, Alvarez-Puebla RA, Rivas G, Liz-Marzán LM. 2012. Surface-enhanced Raman scattering-based detection of the interactions between the essential cell division FtsZ protein and bacterial membrane elements. *ACS Nano* 6:7514–20
153. Sun F, Bai T, Zhang L, Ella-Menye JR, Liu SJ, et al. 2014. Sensitive and fast detection of fructose in complex media via symmetry breaking and signal amplification using surface-enhanced Raman spectroscopy. *Anal. Chem.* 86:2387–94
154. Tsoutsi D, Guerrini L, Hermida-Ramon JM, Giannini V, Liz-Marzán LM, et al. 2013. Simultaneous SERS detection of copper and cobalt at ultratrace levels. *Nanoscale* 5:5841–46
155. Zamarion VM, Timm RA, Araki K, Toma HE. 2008. Ultrasensitive SERS nanoprobes for hazardous metal ions based on trimercaptotriazine-modified gold nanoparticles. *Inorg. Chem.* 47:2934–36
156. Kho KW, Dinish US, Kumar A, Olivo M. 2012. Frequency shifts in SERS for biosensing. *ACS Nano* 6:4892–902
157. Guerrini L, Pazos E, Penas C, Vázquez ME, Mascareñas JL, Alvarez-Puebla RA. 2013. Highly sensitive SERS quantification of the oncogenic protein c-Jun in cellular extracts. *J. Am. Chem. Soc.* 135:10314–17
158. Pazos E, Garcia-Algar M, Penas C, Nazarenus M, Torruella A, et al. 2016. Surface-enhanced Raman scattering surface selection rules for the proteomic liquid biopsy in real samples: efficient detection of the oncoprotein c-MYC. *J. Am. Chem. Soc.* 138:14206–9
159. Tang BC, Wang JJ, Hutchison JA, Ma L, Zhang N, et al. 2016. Ultrasensitive, multiplex Raman frequency shift immunoassay of liver cancer biomarkers in physiological media. *ACS Nano* 10:871–79